



HAL
open science

Muscle parameters estimation based on biplanar radiography

Guillaume Dubois, Philippe Rouch, Dominique Bonneau, Jean-Luc Genisson, Wafa Skalli

► To cite this version:

Guillaume Dubois, Philippe Rouch, Dominique Bonneau, Jean-Luc Genisson, Wafa Skalli. Muscle parameters estimation based on biplanar radiography. *Computer Methods in Biomechanics and Biomedical Engineering*, 2016, 19 (15), pp.1592-1598. <10.1080/10255842.2016.1171855>. <hal-02490636>

HAL Id: hal-02490636

<https://hal.science/hal-02490636v1>

Submitted on 25 Feb 2020

HAL is a multi-disciplinary open access archive for the deposit and dissemination of scientific research documents, whether they are published or not. The documents may come from teaching and research institutions in France or abroad, or from public or private research centers.

L'archive ouverte pluridisciplinaire HAL, est destinée au dépôt et à la diffusion de documents scientifiques de niveau recherche, publiés ou non, émanant des établissements d'enseignement et de recherche français ou étrangers, des laboratoires publics ou privés.



HAL Authorization

Muscle parameters estimation based on biplanar radiography

G. Dubois^a, P. Rouch^a, D. Bonneau^a, J. L. Gennisson^b and W. Skalli^a

^aLBM/Institut de Biomecanique Humaine Georges Charpak, Arts et Metiers ParisTech, Paris, France; ^bInstitut Langevin, Laboratoire Ondes et Acoustique, CNRS UMR 7587, ESPCI ParisTech, INSERM ERL U979, Universite Paris VII, Paris, France

ABSTRACT

The evaluation of muscle and joint forces *in vivo* is still a challenge. Musculo-Skeletal (musculo-skeletal) models are used to compute forces based on movement analysis. Most of them are built from a scaled-generic model based on cadaver measurements, which provides a low level of personalization, or from Magnetic Resonance Images, which provide a personalized model in lying position. This study proposed an original two steps method to access a subject-specific musculo-skeletal model in 30 min, which is based solely on biplanar X-Rays. First, the subject-specific 3D geometry of bones and skin envelopes were reconstructed from biplanar X-Rays radiography. Then, 2200 corresponding control points were identified between a reference model and the subject-specific X-Rays model. Finally, the shape of 21 lower limb muscles was estimated using a non-linear transformation between the control points in order to fit the muscle shape of the reference model to the X-Rays model. Twelfth musculo-skeletal models were reconstructed and compared to their reference. The muscle volume was not accurately estimated with a standard deviation (SD) ranging from 10 to 68%. However, this method provided an accurate estimation the muscle line of action with a SD of the length difference lower than 2% and a positioning error lower than 20 mm. The moment arm was also well estimated with SD lower than 15% for most muscle, which was significantly better than scaled-generic model for most muscle. This method open the way to a quick modeling method for gait analysis based on biplanar radiography.

KEYWORDS

Stereoradiography; muscle; gait analysis; lower limb

1. Introduction

The evaluation of muscle and joint forces *in vivo* is still a challenge; this is why musculo-skeletal models are widely used to simulate and compute forces based on movement analysis. Models have different levels of precision and detail. Most of them are built from a scaled-generic model based on cadaver measurements (Delp and Loan 1995). Magnetic Resonance Images (MRI) are also used to adjust bone geometry, muscle via-points or origin and insertion points (Scheys et al. 2006). Musculo-skeletal models were used to study the influence of joint replacements (Kia et al. 2014) and muscle-tendon transfers (Delp et al. 1994). Neuro-muscular pathologies such as cerebral palsy (CP) were also widely studied (Arnold et al. 2006; Hicks et al. 2007; Scheys et al. 2011; Rezgui et al. 2013).

Authors have underlined the interest of using a subject-specific musculo-skeletal model. Functional roles of the muscles could be well predicted using a scaled-generic model (Correa et al. 2011). However, the level of detail had a major effect on the moment arm (MA)

(Scheys et al. 2008) and on muscle force estimation. The effects of the hip joint center location (Lenaerts et al. 2009), body segment parameters (Pillet et al. 2010; Wesseling et al. 2014) and musculo-skeletal geometry have been studied.

Recently, the development of the low-dose biplanar X-Ray has provided a fast method for the reconstruction of subject-specific bones (Baudoin et al. 2008; Chaibi et al. 2012; Quijano 2013), skin envelope and body segment parameters of the lower limb (Nérot et al. 2015). Hausselle et al. (2012) proposed an original method to obtain a subject-specific musculo-skeletal model of the lower limb in the standing position by combining biplanar X-Ray and MRI. However, the used of MRI is restrictive due to availability, cost and reconstruction time.

Biplanar X-Ray based reconstruction could be a compromise between scaled and fully personalized musculo-skeletal models in the standing positing. The present study explores the level of accuracy that could be obtained using solely low dose biplanar X-Ray.

2. Materials and methods

2.1. Reference model in the standing position

Using both biplanar X-Rays in the standing position and MRI in lying position, the subject-specific musculo-skeletal model in the standing position was computed from the method proposed by [Hauselle et al. \(2012\)](#). This original method is based on a serie of rigid and elastic transformations to register muscle data based on 3D X-Rays reconstruction. The main steps of this method are reminded hereafter:

- (1) Two perpendicular radiographies in the standing position of the lower limb were acquired. 3D geometry in the standing position of bones (pelvis, femurs, tibias), skin envelope ([Chaibi et al. 2012](#); [Quijano 2013](#); [Nérot et al. 2015](#)) and estimation of insertion points coordinate were assessed from biplanar X-Ray using morphorealistic parametric subject specific model.
- (2) 3D model of muscles and skin envelope model in lying position were manually reconstructed from MRI using DPSO method ([Jolivet et al. 2008, 2014](#); [Nordez et al. 2009](#)).
- (3) For both X-Ray and MRI models, corresponding local coordinate systems of each segment were identified based on anatomical landmarks.
- (4) First, a rigid transformation was performed for each segment. The skin envelopes of both models were placed in the same local coordinate system.
- (5) Then, in order to estimate the muscle shape in the standing position, an elastic transformation was applied on each muscle using control points on skin envelope and bones ([Trochu 1993](#)).
- (6) This process resulted in a musculo-skeletal model in the standing position, which combined the 3D models of skin envelope, muscles, bones and insertion points.

The obtained 3D musculo-skeletal model of the lower limb in the standing position was considered as the reference model.

2.2. Geometric musculo-skeletal model in the standing position

By considering solely biplanar X-rays acquisition, a two steps method was considered and presented in details hereafter. First from biplanar X-Rays, 3D reconstruction was performed for skin envelope and bones, including location of muscle insertions. This model was further named bone-envelope model. To estimate the muscle shape, a reference model (bones, skin envelope, origin and insertion points and muscles) was deformed to fit

the subject-specific bone-envelope model. All the parameters which refer to the geometric subject-specific bone-envelope model were designated with a subscripted *be* and all which refer to reference model with a subscripted *ref*.

Step 1 Subject-specific bone-envelope model

The subject-specific bone-envelope model was acquired from low-dose calibrated biplanar radiography ([Dubouset et al. 2005](#)) (EOS®, EOS Imaging, Paris, France). 3D geometry of pelvis, femurs, tibias, fibulas and skin envelope were obtained in the global coordinate system of the X-Ray device using reconstruction methods proposed by [Chaibi et al. \(2012\)](#), [Quijano \(2013\)](#) and [Nérot et al. \(2015\)](#). Virtual Reality Modeling Language was used to describe 3D surface of bony models. Moreover, the coordinates of muscle origin and insertion points were simultaneously obtained ([Hauselle et al. 2012](#)).

A local coordinate system was defined for each bone based on anatomical landmarks identified on the 3D surface:

- Pelvic frame: the centers of acetabular spheres and the sacrum plateau,
- Femoral frame: the centers of condylar spheres and the femoral head center,
- Tibial frame: the middles of the tibial plateaus and the middle of the tibial malleoli.

The following parameters were defined:

- five regions, associated to the following bones respectively, were defined and noted as $B_{ref,i}$ and $B_{be,i}$ for reference and bone-envelope models, with $i = 1 \dots 5$: pelvis, right and left femur, right and left tibia.
- for each region homogeneous matrix was calculated from the global coordinate system to their local coordinate system and noted respectively as $HM_{ref,i}$ and $HM_{be,i}$, with $i = 1 \dots 5$ depending of the bone.
- skin envelopes were respectively noted as SE_{ref} and SE_{be} ,
- origin and insertion points were respectively noted as IP_{ref} and IP_{be} , with $i = 1 \dots 42$ (a single origin and insertion points were considered on 21 muscles).

Step 2 Reference model deformation

In order to fit the reference model to the subject-specific bone-envelope model, corresponding control points (respectively CP_{ref} , CP_{be}) were identified in both models by following steps (Figure 1(a)):

- (1) The nodes of each skin envelope were expressed in the local coordinate system of the associated bony segment (Equations (1) and (2)).

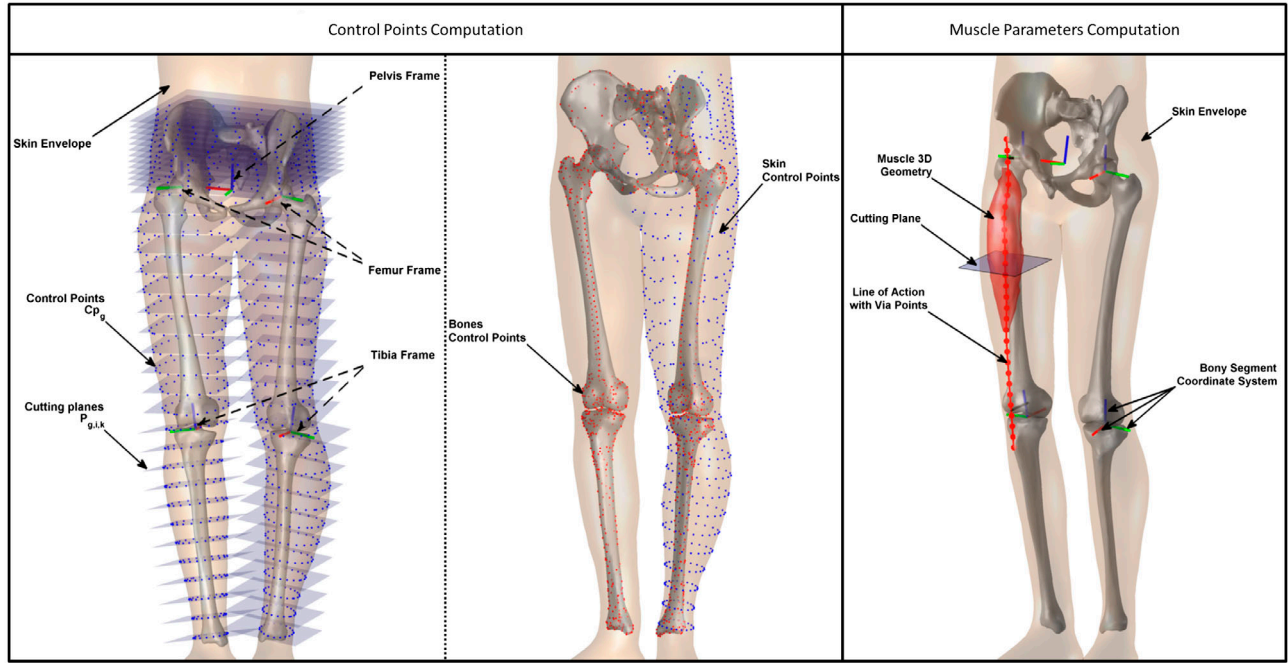


Figure 1. (a) Control points CP_{ref} were equally distributed and computed by cutting skin envelope with planes $P_{ref,i,j,k}$ defined in each bony region. (b) Muscles were cut by planes $P_{ref,i,j,k}$ to evaluate muscle parameters: points, length and cross sectional area.

$$SE_{g\ Loc,i} = HM_{ref,i}^{-1} \cdot SE_{ref} \quad (1)$$

$$SE_{be\ Loc,i} = HM_{be,i}^{-1} \cdot SE_{be} \quad (2)$$

- (2) Local controls points ($CP_{g\ Loc,i}$, $CP_{be\ Loc,i}$) were defined on both models for each bony segment:
 - (a) j planes were equally distributed along the length of the bony segment: $P_{ref,i,j}$ and $P_{be,i,j}$, with $j = 1 \dots 12$ plane number.
 - (b) contours were computed at the intersection between the planes $P_{ref,i,j}$ (respectively $P_{be,i,j}$) and the mesh of the skin envelope $SE_{g\ Loc,i}$ (respectively $SE_{be,i,j}$).
 - (c) on each contour a cubic spline was computed by interpolation of k equally distributed control points $CP_{g\ Loc,i,j,k}$ and $CP_{be\ Loc,i,j,k}$.
- (3) the local control points $CP_{g\ Loc,i,j,k}$ and $CP_{be\ Loc,i,j,k}$ were expressed in the global coordinate system to get the final control points CP_{ref} and CP_{be} (Equations (3) and (4)).

$$\begin{bmatrix} X_{ref,i} \\ Y_{ref,i} \\ Z_{ref,i} \\ 1 \end{bmatrix} = HM_{ref,i} \cdot \begin{bmatrix} X_{g\ Loc,i,j,k} \\ Y_{g\ Loc,i,j,k} \\ Z_{g\ Loc,i,j,k} \\ 1 \end{bmatrix} \quad (3)$$

$$\begin{bmatrix} X_{be,i} \\ Y_{be,i} \\ Z_{be,i} \\ 1 \end{bmatrix} = HM_{ref,i} \cdot \begin{bmatrix} X_{be\ Loc,i,j,k} \\ Y_{be\ Loc,i,j,k} \\ Z_{be\ Loc,i,j,k} \\ 1 \end{bmatrix} \quad (4)$$

Moreover, in order to control the bone shape, 200 control points were added for each bone based on the node of the WRML models. Thus, a total of 2200 control points was defined.

- (4) A Non-linear kriging transformation was applied to each muscle from CP_{ref} to CP_{be} (Trochu 1993) to deform muscles of the reference model to match the subject-specific bone-envelope model.

Thus, an estimation of the muscle shapes of the subject was obtained resulting in a subject-specific musculo-skeletal model of the lower limb in the standing position.

2.3. Method evaluation

Subjects described by Hausselle et al. (2012) were used: four male volunteers with no documented muscular pathology, gave their written consent to participate in this protocol which was approved by the Institutional Ethics Committee (CPP 06036, Paris, France).

The main muscles of the lower limb were considered and divided into three groups:

- pelvic muscles: Gluteus Maximus (GlMa), Gluteus Medius (GlMe), Gluteus Minimus (GlMi) and Iliacus (Ilc).
- thigh muscles: Adductor Brevis (AddB), Adductor Longus (AddL), Adductor Magnus (AddM), Biceps Femoris Long head (BFL), Biceps Femoris Short head (BFS), Gracilis (Gra), Rectus Femoris (RF),

Table 1. Mean and SD of estimated volume and its difference (V_e), estimated muscle length and its difference (ML_e), via points distance (Dist), MA and its difference (Hip MA_e and Knee MA_e) and maximum cross section area and its difference ($CSA_{e,max}$) between estimated muscles and their reference.

Muscle	Volume			V_e (%)			Length			Dist (mm)			Hip MA			Knee MA			Cross section area				
	Value (cm ³)	Mean	SD	Value (%)	Bias	SD	Value (mm)	Mean	SD	Value (mm)	Mean	SD	Value (mm)	Mean	SD	Value (mm)	Mean	SD	Value (cm ²)	Mean	SD	Bias	CSA _e (%)
Pelvis	GIMa	1090	340	4	22	18	213	6	6	8	4	66	6	0	9				72	20	5	20	
	GIMe	353	148	9	41	18	202	3	7	10	3	37	5	6	24			41	17	12	43		
	GIMi	81	24	13	48	12	182	-2	12	9	4	37	5	6	24			13	3	7	29		
	Ilc	149	48	19	63	9	226	0	6	11	6	28	11	21	77			15	4	7	33		
Thigh	AddB	170	38	9	48	7	235	1	3	15	6	77	11	1	27			16	3	2	34		
	AddL	129	78	-24	55	10	234	-1	5	21	11	77	11	1	27			12	6	-23	38		
	AddM	658	102	7	10	6	274	0	3	7	2	85	2	-1	3			43	11	9	26		
	BFL	161	54	16	68	6	466	1	1	15	8	70	3	0	0			48	4	1	4		
	BFS	138	33	0	31	2	461	0	1	18	6							48	4	1	4		
	Gra	87	21	5	29	10	473	0	3	16	14	87	3	-2	9			20	7	4	46		
	RF	320	117	1	31	6	566	0	1	6	3	47	4	1	8			53	8	1	5		
	Sar	140	28	2	17	17	667	1	2	8	2	68	9	3	10	4		20	4	5	4		
	Smem	168	65	10	64	8	457	0	1	9	3	61	2	0	0			40	5	4	9		
	Sten	233	76	3	33	8	522	0	1	9	3	74	3	0	1			28	4	-8	15		
	TFL	50	20	5	26	15	590	0	1	7	2	56	9	1	10			15	4	20	44		
	VI	356	78	1	10	443	5	0	0	7	2							48	3	0	1		
	VL	999	285	2	29	430	5	0	1	6	2	47	6	3	6			47	6	3	6		
	VM	656	261	15	60	415	5	0	2	11	4							39	7	-10	13		
	Calf	GL	187	47	-6	18	13	480	0	2	18	13	27	6	7	35			13	3	-1	22	
		GM	169	60	13	40	14	480	1	3	23	18	24	3	4	17			12	4	9	22	
Sol		508	161	11	46	8	376	0	2	8	2	33	10	10	10			33	10	10	44		

Sartorius (Sar), Semimembranosus (Smem), Semitendinosus (Sten), Tensor Fascia Latae (TFL), Vastus Intermedius (VI), Vastus Lateralis (VL) and Vastus Medialis (VM).

- calf muscles: Gastrocnemius Lateralis (GL), Gastrocnemius Medialis (GM) and Soleus (Sol).

The subject-specific musculo-skeletal model in the standing position of each subject was reconstructed using the method described in Section 2.3. One by one, each reference model was used to estimate the muscle shape of the other three. Thus, $4 \times 3 = 12$ estimated models were constructed. The estimated muscle shapes were compared to their reference.

2.4. Parameters studied

To evaluate the accuracy of the method, the estimated muscles were compared to their references. The bias (mean) and the reliability (SD) were used to evaluate the difference of the 24 estimated muscles for the following parameters (Figure 1(b)):

- Volume.
- Maximum Cross Sectional Area (CSA): each muscle was sectioned on 50 planes equally spaced along the length of the muscle and the maximum CSA was retained.
- Muscle length: a Line of Action (LoA) was defined as a spline of 50 via points from the origin to the insertion points passing through the center of each cross section. The muscle length was computed as the sum of the distance between via points.
- Distance between via points: RMS of the distance between corresponding via points of both models.
- MA: the distance between the LoA and the joint centers. The center of the hip joint was defined as the center of the sphere fitting the femoral head and the center of the knee joint was defined as the middle of the centers of the spheres fitting the posterior part of the condyles.

3. Results

3.1. Evaluation of the method

Bias (Table 1) Most muscle volumes were overestimated with a bias between 0 and 19%, except for the gastrocnemius lateralis (−6%) and the adductor longus (−24%). Muscle length was estimated with a bias of between −1 and 3%. The MA of the hip joint was over estimated for the iliacus with a bias of 21%; however the bias was between −2 and 6% for the other muscles. For most muscles, the MA in knee joint was estimated with a bias of between −10 and 7%, except for the Semitendinosus

(20%). Most muscles had an over-estimated CSA, which was positive up to 16%, except for the gastrocnemius lateralis (−1%) and the adductor longus (−23%).

Standard Deviation (SD) (Table 1) The muscle volume SD ranged from 10% for the vastus intermedialis to 68% for the biceps femoris long head. The muscle length SD was lower than 12% for all muscles. The SD of MA in hip joint ranged from 1% for the semitendinosus to 77% for the iliacus. The SD of the MA in knee joint ranged from 1% for the tensor fascia latae to 46% for the semitendinosus. The SD of the CSA ranged from 15% for the adductor magnus and 183% for the adductor longus.

The Rmusculo-skeletal of the via point distances ranged from 6 ± 2 mm for the vastus intermedialis to 23 ± 18 mm for the gastrocnemius medialis (Table 1). Most muscles were estimated with a mean lower than 15 mm.

4. Discussion

This study proposed an original method to quickly access a subject-specific musculo-skeletal model of the lower limb in the standing position based on low-dose biplanar X-Ray. The reconstruction time was about 30 min vs. about 2.5 h with an MRI based method combining MRI and X-Ray to obtain a subject-specific MS model in the standing position (Hausselle et al. 2012). Bones and skin envelopes were subject-specific, origin and insertion points were estimated and muscle shapes were computed from reference model deformation.

This original method produced an accurate estimation of muscle LoA. Indeed, the LoA of thigh and calf muscles were well estimated with a SD of the muscle length lower than 5%. Muscles were also well positioned with the RMS of the via point distances under 20 mm for the majority of the muscle. The gluteus muscles were more difficult to estimate because they are superficial, thin and short; thus, the LoA was more influenced by the deformation, especially the muscle length error in percent. Otherwise, only a single LoA was considered here, while Arnold et al. (2006), Martelli et al. (2013) had decomposed them in several bodies. This choice was made in order to simplify the comparison between models. Calf muscle error was mainly due to the insertion position, which was estimated, because the Achilles tendon position was unknown. Despite that, results were better than those provided using a scaled-generic model. Indeed, Scheys et al. (2008) reported a length difference of around 20% between the reference and personalized models.

The MA was also well estimated with a SD lower than 15% for most muscles compared to Scheys et al. (2006) and Scheys et al. (2008), which shows a difference

Table 2. MAs in hip and knee joints computed for the proposed method and generic-scaled model compared to the method proposed by Hauselle et al. (2012).

	Muscle	Proposed method		Scaled-generic model	
		Bias (%)	SD (%)	Bias (%)	SD (%)
Hip	AddB*	1	27	-34	14
	AddL*	1	27	-34	6
	AddM*	-1	3	-28	27
	BFL	0	0	-1	6
	GlMa	0	9	2	14
	GlMe*	6	24	-9	7
	GlMi*	6	24	-25	9
	Gra	-2	9	-5	5
	Ilc*	21	77	-5	32
	RF*	1	8	15	19
	Sar*	3	10	20	20
	Smem*	0	0	-8	6
	Sten*	0	1	4	8
	TFL	1	10	4	10
Knee	BFL	1	4	0	12
	BFS*	1	4	9	9
	Gra	4	46	-8	39
	RF*	1	5	-14	14
	Sar*	4	9	-6	17
	Smem*	-8	15	16	39
	Sten	20	44	7	38
	TFL*	0	1	18	12
	VI*	3	6	-7	7
	VL	3	6	-3	20
	VM	-10	13	-7	7

* indicates a lower significant difference between proposed method and generic-scaled model ($p < 0.05$).

between the reference and personalized models of over 20% for most muscles and up to 100% for some muscles. For most muscles, the use of a reference model including a tendon pathway could better predict MA. Indeed, a tendon pathway was estimated between the belly part ends and the insertion point by a spline, which could be different to the real one. The tendon pathway could not segmented due to the lack of visibility on MRI for some muscles.

The presented model must be compared with the scaled-generic model. Table 2 summarizes the difference of the MA in hip and knee joints computed for the presented study and for the scaled-generic model compared to the reference model (Hauselle et al. 2012). The proposed method significantly increased the accuracy of MA computation for Adductors, GlMe, GlMi, RF, Sar, Smem in the hip joint and BFS, RF, Sar, Smem, TFL in the knee joint.

The muscle volume was less accurately estimated. The non-linear deformation from the reference model to the subject-specific musculo-skeletal model allowed an estimate of muscle belly in the transverse plane. The individual height variability of muscle belly length was not accurately estimated. Thus, CSA was better estimated than muscle volume ($p < 0.03$). The proposed method had not taken into account subject fat thickness, this was the main limitation. The closer the fat thickness is to

the reference model, the more accurate the estimation is.

The choice of the reference model will affect the estimation of the muscle shape: if the reference model is close to the subject, the estimation may be more accurate. Generally, the reference model could be an average subject of a large database in order to cover the largest morphology range. In our case, we only have a database of four subjects and by considering each one as the reference model to estimate the other three, the sensitivity of the reference model was investigated.

The main limitation was the number of subjects. An increase of the database would increase the relevance of the estimation. However, the first presented results highlighted the good potential of the method. A further large scale study, which includes information on fat thickness and gait analysis, will be performed, this should yield an improvement of the database and of the estimation.

This study proposed a fast method for subject-specific skeletal modeling of the lower limb in the standing position, with a good estimation of the muscle line of action. The bones and skin envelope were subject-specific and most muscle parameters were more accurately estimated than with scaling. This method open the way to a quick modeling method for gait analysis based on biplanar radiography.

Acknowledgements

The authors wish to thank Lee-Anne Welgemoed for the English correction.

Disclosure statement

The authors do not have any conflicting financial interests.

References

- Arnold AS, Liu MQ, Schwartz MH, Ounpuu S, Delp SL. 2006. The role of estimating muscle-tendon lengths and velocities of the hamstrings in the evaluation and treatment of crouch gait. *Gait Posture*. 23:273–281.
- Baudoin A, Skalli W, de Guise JA, Mitton D. 2008. Parametric subject-specific model for in vivo 3D reconstruction using bi-planar X-rays: Application to the upper femoral extremity. *Med Biol Eng Comput*. 46:799–805.
- Chaibi Y, Cresson T, Aubert B, Hausselle J, Neyret P, Hauger O, de Guise JA, Skalli W. 2012. Fast 3D reconstruction of the lower limb using a parametric model and statistical inferences and clinical measurements calculation from biplanar X-rays. *Comput Methods Biomech Biomed Eng*. 15:457–466.
- Correa TA, Baker R, Graham HK, Pandey MG. 2011. Accuracy of generic musculoskeletal models in predicting the functional roles of muscles in human gait. *J Biomech*. 44:2096–2105.
- Delp SL, Loan JP. 1995. A graphics-based software system to develop and analyze models of musculoskeletal structures. *Comput Biol Med*. 25:21–34.
- Delp SL, Ringwelski DA, Carroll NC. 1994. Transfer of the rectus femoris: effects of transfer site on moment arms about the knee and hip. *J Biomech*. 27:1201–1211.
- Dubouset J, Charpak G, Dorion I, Skalli W, Lavaste F, Deguise J, Kalifa G, Ferey S. 2005. A new 2D and 3D imaging approach to musculoskeletal physiology and pathology with low-dose radiation and the standing position: The EOS system. *Bulletin de l'Académie nationale de médecine*. 189:287–300.
- Hausselle J, Assi A, El Helou A, Jolivet E, Pillet H, Dion E, Bonneau D, Skalli W. 2012. Subject-specific musculoskeletal model of the lower limb in a lying and standing position. *Biomed Eng: Comput Methods Biomech*. 17:480–487.
- Hicks J, Arnold A, Anderson F, Schwartz M, Delp S. 2007. The effect of excessive tibial torsion on the capacity of muscles to extend the hip and knee during single-limb stance. *Gait Posture*. 26:546–552.
- Jolivet E, Daguet E, Pomero V, Bonneau D, Laredo JD, Skalli W. 2008. Volumic patient-specific reconstruction of muscular system based on a reduced dataset of medical images. *Comput Methods Biomech Biomed Eng*. 11:281–290.
- Jolivet E, Dion E, Rouch P, Dubois G, Charrier R, Payan C, Skalli W. 2014. Skeletal muscle segmentation from MRI dataset using a model-based approach. *Comput Methods Biomech Biomed Eng: Imaging Visual*. 2:138–145.
- Kia M, Stylianou AP, Guess TM. 2014. Evaluation of a musculoskeletal model with prosthetic knee through six experimental gait trials. *Med Eng Phys*. 36:335–344.
- Lenaerts G, Bartels W, Gelaude F, Mulier M, Spaepen A, Van der Perre G, Jonkers I. 2009. Subject-specific hip geometry and hip joint center location affects calculated contact forces at the hip during gait. *J Biomech*. 42:1246–1251.
- Martelli S, Calvetti D, Somersalo E, Viceconti M, Taddei F. 2013. Computational tools for calculating alternative muscle force patterns during motion: A comparison of possible solutions. *J Biomech*. 46:2097–2100.
- Nérot A, Choisine J, Amabile C, Travert C, Pillet H, Wang X, Skalli W. 2015. A 3D reconstruction method of the body envelope from biplanar X-rays: Evaluation of its accuracy and reliability. *J Biomech*. 48:4322–4326.
- Nordez A, Jolivet E, Südhoff I, Bonneau D, de Guise JA, Skalli W. 2009. Comparison of methods to assess quadriceps muscle volume using magnetic resonance imaging. *J Magn Reson Imaging*. 30:1116–1123.
- Pillet H, Bonnet X, Lavaste F, Skalli W. 2010. Evaluation of force plate-less estimation of the trajectory of the center of pressure during gait. Comparison of two anthropometric models. *Gait Posture*. 31:147–152.
- Quijano S, Serrurier A, Aubert B, Laporte S, Thoreux P, Skalli W. 2013. Three-dimensional reconstruction of the lower limb from biplanar calibrated radiographs. *Med Eng Phys*. 35:1703–1712.
- Rezgui T, Megrot F, Marin F. 2013. Musculoskeletal modelling of cerebral palsy children: sensitivity analysis of musculoskeletal model parameter's values for gait analysis. *Comput Methods Biomech Biomed Eng*. 16(sup1):155–157.
- Scheys L, Desloovere K, Spaepen A, Suetens P, Jonkers I. 2011. Calculating gait kinematics using MR-based kinematic models. *Gait Posture*. 33:158–164.
- Scheys L, Jonkers I, Loeckx D, Maes F, Spaepen A, Suetens P. 2006. Biomedical simulation. Lecture notes in computer science, Vol. 4072, Springer: Berlin Heidelberg.
- Scheys L, Van Campenhout A, Spaepen A, Suetens P, Jonkers I. 2008. Personalized MR-based musculoskeletal models compared to rescaled generic models in the presence of increased femoral anteversion: Effect on hip moment arm lengths. *Gait Posture*. 28:358–365.
- Trochu F. 1993. A contouring program based on dual kriging interpolation. *Eng Comput*. 9:160–177.
- Wesseling M, de Groote F, Jonkers I. 2014. The effect of perturbing body segment parameters on calculated joint moments and muscle forces during gait. *J Biomech*. 47:596–601.